Conducting-Polymer Microcontainers: Controlled Syntheses and Potential Applications**

By *Vardhan Bajpai*, *Pingang He*, and *Liming Dai**

We have demonstrated the controlled synthesis of conducting-polymer microcontainers through the electrochemical generation of surfactant (i.e., β-naphthalenesulfonic acid, β-NSA)-stabilized H_2 gas bubbles on the working electrode, followed by electrochemical polymerization of pyrrole around the wall of the "soap-bubble" template. It was noticed that the density, shape, and wall thickness of the polypyrrole microcontainers thus prepared could be regulated by controlling the electrochemical potential applied for the generation of H_2 gas and the experimental conditions (e.g., the surfactant concentration, number of the cyclic voltammetric scanning) for the electropolymerization of pyrrole. By pre-patterning the working electrode surface with non-conducting polymers using microcontact printing (μCP) or plasma patterning, we have also produced conducting-polymer microcontainers in a patterned fashion. Furthermore, potential applications of the patterned and non-patterned conducting-polymer microcontainers have been demonstrated; for example, through the encapsulation of appropriate fluorescence-labeled molecules (e.g., fluorescein cadaverin) into the conducting-polymer microcontainers by sealing their opened mouths with sequential electropolymerization of pyrrole. The resulting closed microcontainers could then be used for controlled releases.

1. Introduction

Recent advances in nanoscience and nanotechnology have aided the development of micro- and nanostructured polymers, which in turn has opened up novel fundamental and applied frontiers. Consequently, various methods have been devised for preparing a wide range of micro- or nanostructured polymers for advanced applications.[1] Examples include the use of polymer particles for drug delivery,[2] polymer fibers as conducting wires,[3] polymer thin films, and periodically structured polymeric materials for photonic device applications.[4] Of particular interest, conducting polymer micro- or nanofibers and/or -tubes have been synthesized within the pores of porous substrates.[5] Although the so-called template synthesis can produce monodispersed polymeric fibers or tubes with a well-defined geometry, a rather tedious post-synthesis process for removal of the template is often necessary in order to release the micro- or nanostructured polymers.[6] Very recently, Shi and co-workers[7] reported the electrochemical deposition of template-free polypyrrole microcontainers onto "soap bubbles" associated with the O_2 gas released from electrolysis of H_2O in an aqueous solution of β-naphthalenesulfonic acid (β-NSA), which acts as both the surfactant and electrolyte. The conducting-polymer microcontainers thus produced have been demonstrated to display unusual morphologies and have a large number of potential applications. In view of the fact that the direct generation of O_2 gas on the working electrode under a relatively high positive potential (> 0.8 V) could have a detrimental over-oxidation effect, we started the electrochemical polymerization of polypyrrole microcontainers by releasing H_2 (electrolysis of H_2O) around the working electrode under a negative potential. The newly released H_2 gas bubbles were stabilized by the anionic surfactant molecules in the solution and assembled onto the working electrode under a positive potential to act as the "soap-bubble" template for the formation of conducting-polymer microcontainers. Unlike the previously reported "soap-bubble" template synthesis, which produces no polypyrrole microcontainers at the potentials below 0.8 V,[7] the modified method should allow the formation of conducting-polymer microcontainers on the working electrode even at a relatively low potential, as we shall see later. In conjugation with various surface-patterning techniques,[8] we have recently applied the modified "soap-bubble" template synthesis to the electrochemical deposition of conducting-polymer microcontainers both in patterned and non-patterned fashions. Here, we report the use of the "soap-bubble" template synthesis for making polypyrrole microcontainers with controlled structures and packing patterns. The formation of polypyrrole microcontainer capsules for potential applications in controlled releases is also demonstrated by closing the microcontainers through sequential electropolymerization(s) in an appropriate solution containing species to be encapsulated, followed by collapsing the microcontainers to release the encapsulated reagents.

[*] Prof. L. Dai, V. Bajpai, Dr. P. He
Department of Polymer Engineering
College of Polymer Science and Polymer Engineering
The University of Akron, Akron, OH 44235-0301 (USA)
E-mail: ldai@uakron.edu

[**] The authors are grateful for a useful discussion with Professor G. Shi at Tsinghua University. We also thank Prof. S. Huang in Kent State University and Prof. Jun Hu in The University of Akron for their assistance.

2. Results and Discussion

In a typical experiment, cyclic voltammetric scanning was performed in an aqueous solution of 0.25 M pyrrole and 0.4 M β-naphthalenesulfonic acid sodium salt (β-NSA, 99 %, Acros), which was pre-degassed with a pure nitrogen gas flow for

 DOI: 10.1002/adfm.200304489

15 min and subsequently maintained under a slight overpressure throughout the electrochemical process. In order to generate H_2 bubbles on the working electrode surface, the scan potential window was set from –1.0 to –1.6 V for the first cycle. Subsequently, the potential window was changed to the range of 0.5 to 1.1 V for the next several cycles for electrochemical polymerization of pyrrole around the "soap bubbles" on the working electrode. Without the first cycle over the negative potential window for the generation of H_2 bubbles, we observed no microcontainer formation, even using a very wide potential window from –0.8 to 1.1 V for the electropolymerization of pyrrole, indicating that the H_2 gas is responsible for the "soap-bubble" template syntheses of conducting-polymer microcontainers in this study.

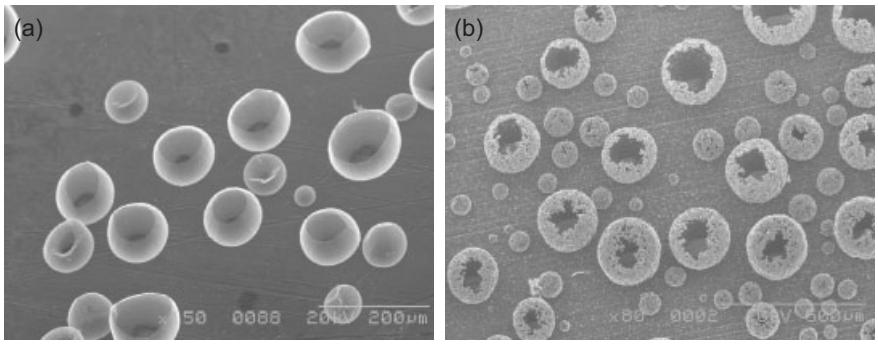

Figure 1. SEM images of polypyrrole microcontainers prepared by electrochemical polymerization in the voltage window of a) 0.5 to 1.1 V, scan rate of 100 $mV s^{-1}$, 5 cyclic voltammogram scans, and 0.2 M β-NSA; and b) 0.5 to 0.75 V, scan rate of 100 $mV s^{-1}$, 10 cyclic voltammogram scans, and 0.4 M β-NSA. In both cases, the aqueous electrolyte solution contains 0.25 M pyrrole and the bubble generation voltage window is –1.0 to –1.7 V.

Figures 1a,b show typical scanning electron micrographs (SEMs) of the polypyrrole microcontainers prepared by electrochemical polymerization of pyrrole on the "soap-bubble" template above and below a potential of 0.8 V, respectively. Although microcontainers with different sizes have been observed, the majority of the microcontainers formed under this particular experimental condition have a budlike shape. Comparing Figure 1a with Figure 1b indicates that the formation of conducting-polymer microcontainers at potentials above 0.8 V not only proceeds faster but also leads to a smoother surface. There are also more small containers seen in Figure 1b than in Figure 1a, suggesting the possible shrinkage of the "soap bubbles" through the leakage of H_2 gas during the slow polymerization process. Based on the above findings, we will focus below on the fast microcontainer formation process at potentials above 0.8 V.

By changing the electrochemical polymerization conditions, it was found that polypyrrole microcontainers of different shapes could be produced. For instance, microbowls like the one shown in Figure 2a were produced at a low polymerization potential (0.5 to 0.9 V) for a small number of cycles (2 cycles). If the polymerization potential was increased up to 1.1 V, budlike (Fig. 2b) and lantern-like (Fig. 2c) polypyrrole microcontainers formed with an increased scanning rate. It was also found that the wall thickness of the microcontainers depended strongly on the concentration of pyrrole in the solution. Comparison of Figures 2a,b with Figure 2c indicates that microcontainers with a thicker wall form at a higher concentration of pyrrole while thinner-walled microcontainers with a smooth surface can be produced from the solution of a lower pyrrole concentration. However, it is difficult (if not impossible) to control the caliber and height of the resulting microcontainers as they are, most likely, controlled by the growth kinetics of "soap bubbles" on the electrode surface.

We additionally found that the potential used for generating H_2 gas also had an influence on the density of resultant microcontainers. As can be seen in Figure 3, the lower the negative potential for the H_2 gas generation, the more densely packed polypyrrole microcontainers formed on the working electrode due to the formation of more "soap bubbles" on the working electrode surface at a lower H_2 generation potential.

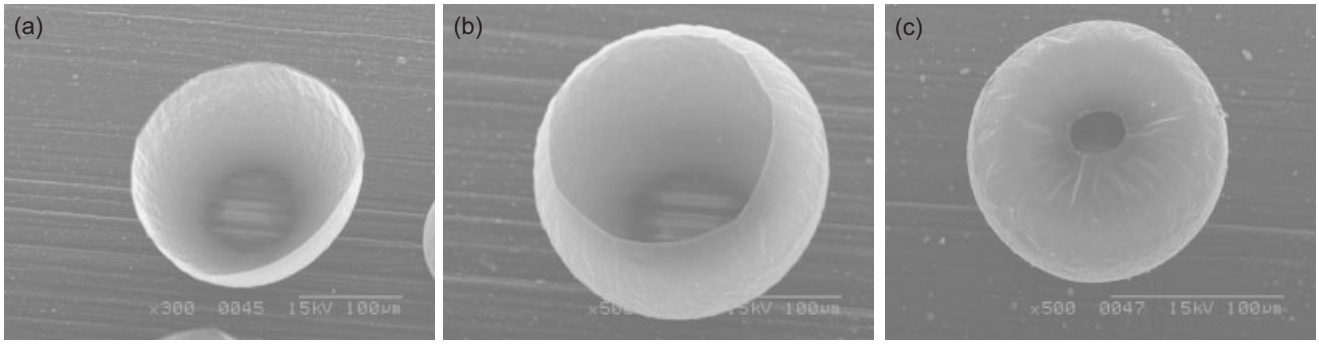

Figure 2. SEM images of polypyrrole microstructures formed by cyclic voltammetric polymerization under different electropolymerization conditions; a) 0.5–0.9 V, scan rate 20 $mV s^{-1}$, 2 cycles; b) 0.5–1.1 V, scanning rate 20 $mV s^{-1}$, 3 cycles; c) 0.5–1.1 V, scan rate 100 $mV s^{-1}$, 3 cycles. Potential window of generating air bubbles is from –1.0 to –1.65 V for one cycle. Electrolyte aqueous solutions are 0.25 M pyrrole and 0.4 M β-NSA (a,b) and 0.5 M pyrrole and 0.4 M β-NSA (c), respectively (scale bars: 100 μm).

ADVANCED FUNCTIONAL MATERIALS

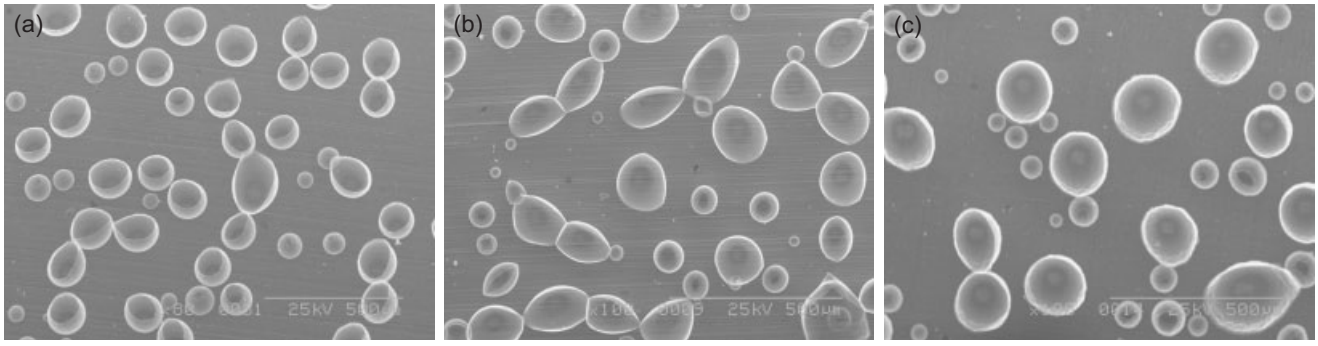

Figure 3. SEM images of polypyrrole microstructures formed by cyclic voltammetric polymerization over a 0.5 to 1.1 V potential window, scanning rate of 20 mV s^{-1}, 3 cycles. Potential windows for generating soap bubbles are a) from –1.0 to –1.65 V; b) from –1.0 to –1.4 V; c) from –1.0 to –1.3 V for the first cycle. The aqueous electrolyte solutions contain 0.4 M β-NSA and a) 0.25 M pyrrole or b,c) 0.5 M pyrrole (scale bars: 500 μm).

The effect of the β-NSA concentration on the size, morphology, and packing density of the resulting polypyrrole microcontainers can be seen in Figure 4. As shown in Figure 4, the formation yield of the microcontainers increased with increasing β-NSA concentration. Higher concentrations of β-NSA also led to the formation of bigger and/or more closed microcontainers. These observations can be rationalized in view of the fact that the more β-NSA molecules that were present in the electrolyte solution the more stable big "soap bubbles" could form on the working electrode.

In addition to the effects of the β-NSA concentration and electrochemical potentials for both the H_2 gas generation and polypyrrole deposition discussed above, Figure 5 shows SEM images taken at different stages during the polypyrrole microcontainer growth. While Figure 5a shows the formation of the microcontainer base on the electrode surface, Figure 5b reveals that the base structure evolved into a bowl-like microcontainer as the number of the cyclic voltammetric scan was increased. Further increase in the cycle number led to the formation of lantern-like (Figs. 5c,d) and eventually fully closed (Fig. 5e) microcontainers.

To elucidate the chemical structure of the polypyrrole microcontainer sample, we carried out the Fourier-transform infrared (FTIR) spectroscopic measurements, using a conventional polypyrrole film electropolymerized in an aqueous solution of $NaClO_4$ as reference. As can be seen in Figure 6, the microcontainer sample (curve b of Fig. 6) shows a similar spectrum as that of polypyrrole prepared with the perchlorate electrolyte without the formation of microcontainers (curve a of Fig. 6). Both of the spectra show characteristic absorption peaks corresponding to the N–H/C=C bending vibration and C–N stretching modes of the pyrrole ring at 1439 and 1144 cm^{-1}.[9] Also, the C=C/C–C stretching vibration absorption peak can be seen at 1518 cm^{-1} in both curves of Figure 6.

However, comparing curve a to curve b in Figure 6 reveals three new absorption peaks for the microcontainer sample. The new absorption peaks at 1605 and 1230 cm^{-1} seen in curve b of Figure 6 can be attributed to the naphthalene ring and $-SO_3^-$ group of the dopants,[10] respectively. These results suggest that the microcontainers were made of slightly doped polypyrrole. The third new absorption peak seen at 1742 cm^{-1} in curve b of Figure 6 arises, most probably, from the carbonyl group, indicating that the polypyrrole microcontainers might have been slightly overoxidized during the growth process, as is the case with the previous work.[7]

Techniques for region-specific control of nano- or microstructures on surfaces are of paramount importance to a large variety of potential applications ranging from sensing to optoelectronics. Insights gained from the above studies on the effects of synthetic conditions on the microcontainer formation

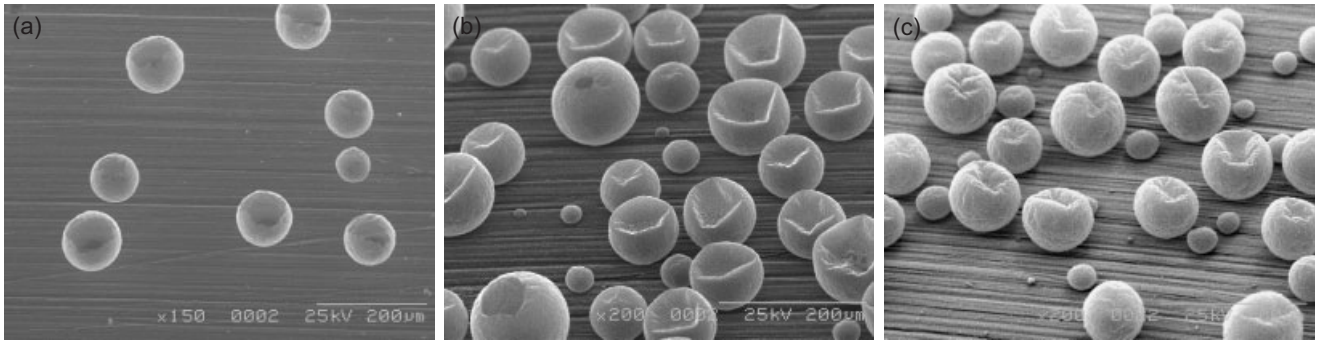

Figure 4. SEM images of polypyrrole microstructures formed by cyclic voltammetric polymerization over a 0.5 to 1.1 V potential window for the electrochemical deposition, –1.0 to –1.7 V potential window for generating soap bubbles for the first cycle and scan rate of 100 mV s^{-1} for 3 cycles. The electrolyte aqueous solutions contain 0.25 M pyrrole and various β-NSA concentrations: a) 0.1 M, b) 0.2 M, and c) 0.3 M (scale bars: 200 μm).

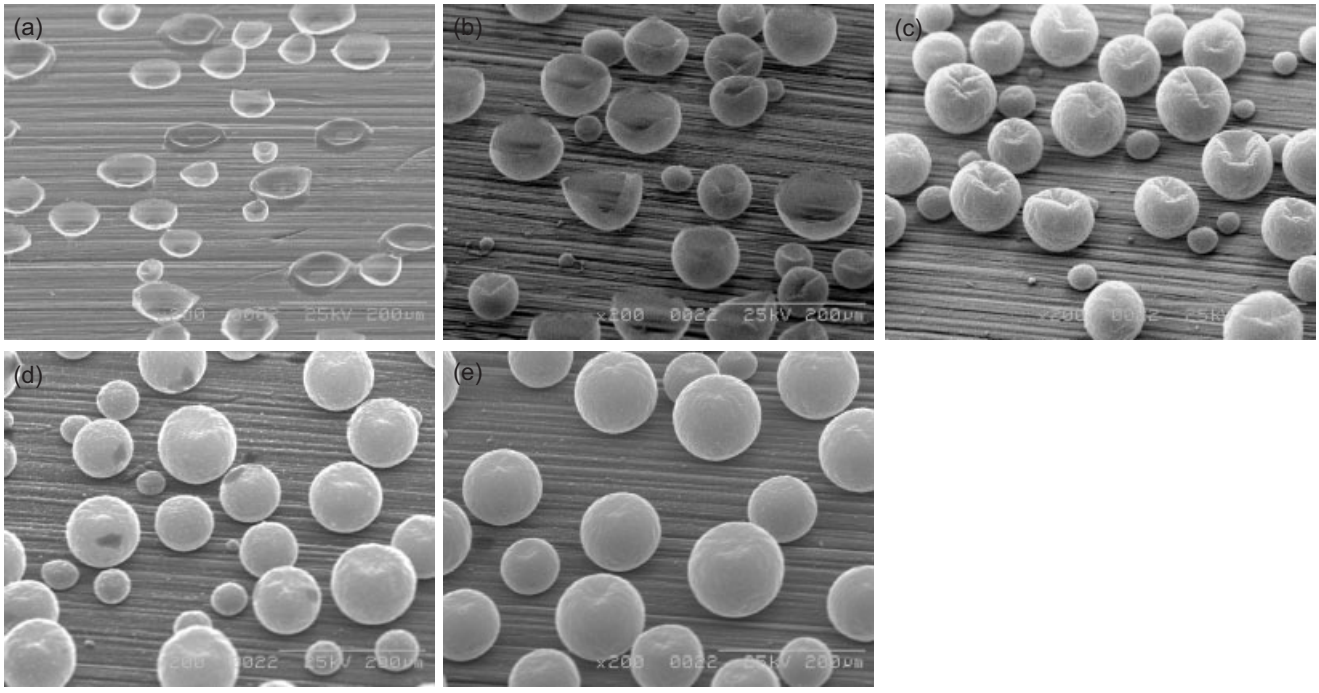

Figure 5. SEM images of polypyrrole microstructures formed by cyclic voltammetric polymerization over a 0.5 to 1.1 V potential window for the electrochemical deposition, –1.0 to –1.7 V potential window for generating soap bubbles for the first cycle, and scan rate of 100 $mV\,s^{-1}$ at various cycle numbers: a) 1 cycle, b) 2 cycle, c) 3 cycle, d) 4 cycle, and e) 5 cycle. The electrolyte aqueous solution contains 0.25 M pyrrole and 0.3 M β-NSA (scale bars: 200 μm).

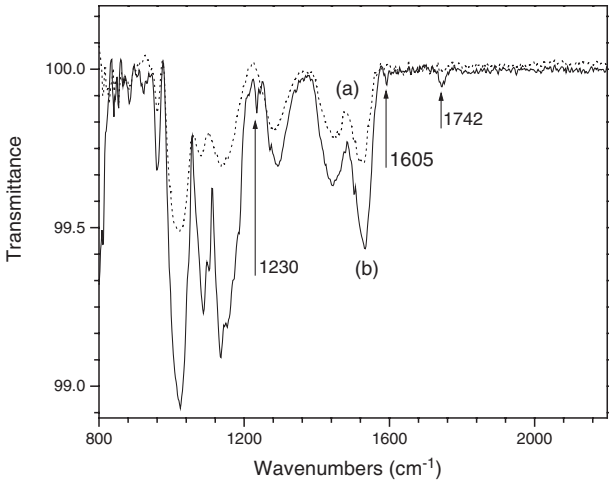

Figure 6. FTIR spectra of a) a polypyrrole film electropolymerized in an aqueous solution of $NaClO_4$ and b) polypyrrole microcontainers electropolymerized in an aqueous solution of β-NSA.

facilitate our approaches to the patterned growth of polypyrrole microcontainers on electrodes pre-patterned with a non-conducting layer by various patterning techniques, including microcontact printing (μCP) and plasma patterning.[8,11] We have previously used the plasma patterning method for preparing patterned conducting polymers by first depositing a thin patterned non-conducting plasma polymer layer (e.g., *n*-hexane plasma film) onto a metal-sputtered electrode, followed by electropolymerization of appropriate monomers (e.g., pyrrole) within the regions not covered by the patterned plasma-polymer layer.[12] In this study, we found that both the plasma patterning method and the μCP technique can be used to pattern the stainless steel electrode with non-conducting polymers for patterned growth of polypyrrole microcontainers in the non-conducting polymer-free regions.

Figures 7a,b schematically show the steps for the patterning processes by the μCP and plasma method, respectively. Prior to the patterning, all of the stainless steel electrodes were cleaned by an aqueous solution of HNO_3 (1:1 v/v, H_2O/HNO_3) using ultrasonication for 30 min, followed by thorough washing with distilled water and acetone. For the μCP patterning (Fig. 7a), a drop of the polyvinyl chloride (PVC) solution in chloroform was spread out on a clean stainless steel electrode and region specifically confined with a poly(dimethylsioxane) (PDMS) stamp by pressing. After drying at room temperature for about 1 min, polymer patterns were observed upon removal of the PDMS stamp. The PVC patterns on the stainless steel surface thus produced then act as a physical mask for the patterned growth of the polypyrrole microcontainers. Alternatively, non-conducting plasma polymer patterns can be produced on the stainless steel electrode surface by plasma polymerization of an appropriate monomer (e.g. *n*-hexane at 150 KHz and 0.3 torr for 2 min) through a mask (Fig. 7b). These electrodes with a pre-patterned non-conducting polymer layer either by the μCP or plasma method were then used for region-specific electrochemical deposition of the polypyrrole microcontainers.

ADVANCED FUNCTIONAL MATERIALS

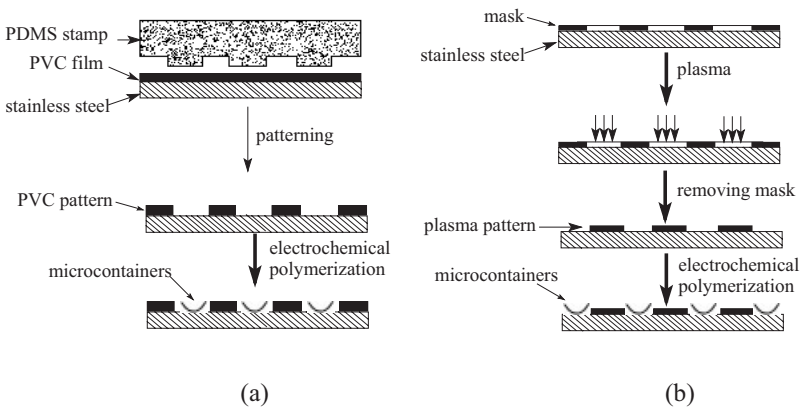

Figure 7. Schematic illustration of the procedures for fabricating patterns of polypyrrole microcontainers by a) μCP and b) plasma patterning.

Figure 8a shows a typical SEM image of the microcontainer patterns generated on a stainless steel electrode by the μCP method. The darker regions with relatively thick strips seen in Figure 8a indicate the presence of the patterned PVC coating and the polypyrrole microcontainers are clearly confined to the PVC-free regions. Figure 8b reproduces a SEM image for polypyrrole microcontainer patterns produced by the plasma patterning technique. As can be seen in Figure 8, polypyrrole microcontainers can be electrodeposited within specific regions on electrodes pre-patterned with non-conducting polymers prepared by different patterning methods. The patterned conducting polymer microcontaniners thus prepared may find a wide range of applications, including in controlled release, sensing, and optoelectronic devices.

To demonstrate the potential applications of the polypyrrole microcontainers, we have measured the cyclic voltammetric response of a polypyrrole film deposited with (curve a of Fig. 9) and without (curve b of Fig. 9) microcontainers. Figure 9 clearly shows a much stronger redox response for the microcontainer-deposited electrodes due to the large surface areas associated with the microcontainers. As conducting polymers have been long investigated as transducers in chemical and biosensors,[13] Figure 9 reveals additional advantages for the use of the conducting-polymer microcontainers for sensing applications.

These conducting-polymer microcontainers with a large surface are also good candidates for controlled-release applications. One of the major challenges for such practical applications is to close the "mouth" of the microcontainer so that species to be released can be sealed inside the microstructures. Apart from the as-synthesized closed microcontainers prepared by electropolymerization with a sufficient number of cyclic voltammetric scans (see Fig. 5), we found that the opened polypyrrole microcontainers could be sealed by further polymerization of pyrrole on the microcontainer "mouth". This observation indicates that there is considerable potential for using the microcontainers to encapsulate various objects.

Figure 10 shows SEM images of the semi-closed polypyrrole microcontainers before (Fig. 10a) and after (Figs. 10b,c) being subjected to the subsequent polymerization(s). While Figure 10a reproduces an SEM image of the as-prepared polypyrrole microcontainers, 2 and 5 additional cyclic voltammetric scans were found to seal "mouths" of the resulting polypyrrole microcontainers partially (Fig. 10b) and fully (Fig. 10c), respectively.

To demonstrate the capacity of the conducting-polymer microcontainers for encapsulation of foreign species, we have

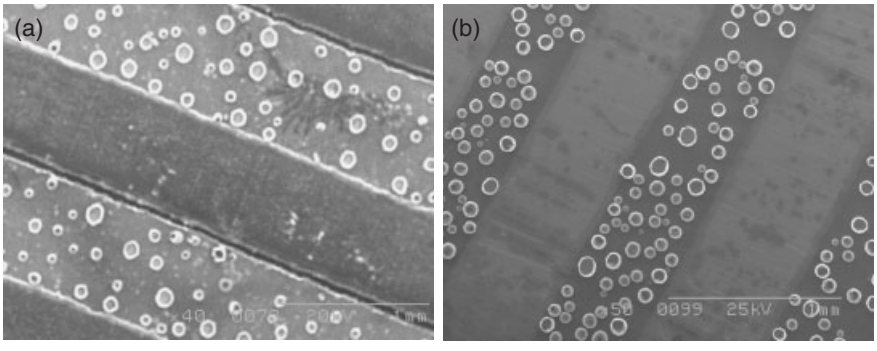

Figure 8. SEM images of polypyrrole microcontainer patterns obtained by a) μCP and b) plasma patterning. The parameters for preparing polypyrrole microcontainers are a) for generating the soap-bubble template: voltammetric scanning from –1.0 to –1.65 V, scanning rate 20 $mV s^{-1}$, 1 cycle; and for electropolymerization: voltammetric scanning from 0.5 to 1.1 V, scanning rate 20 $mV s^{-1}$, 3 cycles in the electrolyte aqueous solution of 0.5 M pyrrole and 0.4 M β-NSA; b) for generating the soap-bubble template: voltammetric scanning from –1.0 to –1.65 V, scanning rate 20 $mV s^{-1}$, 1 cycle, and for electropolymerization: voltammetric scanning from 0.5 to 1.1 V, scanning rate 50 $mV s^{-1}$, 3 cycles in the electrolyte aqueous solution of 0.25 M pyrrole and 0.4 M β-NSA (scale bars: 1.0 mm).

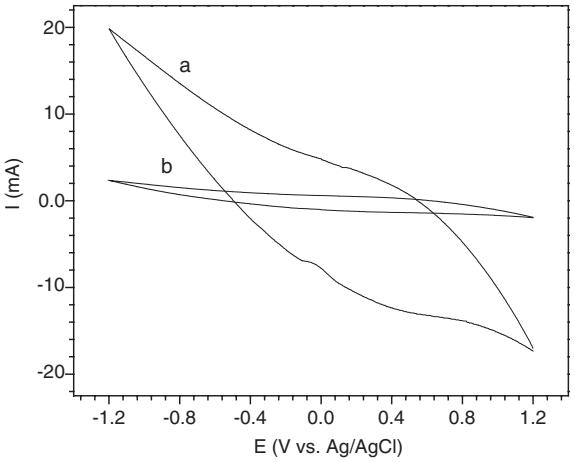

Figure 9. Cyclic voltammograms of a polypyrrole film with a) microcontainers and b) a flat polypyrrole film in an aqueous solution of $NaClO_4$ (0.1 M) at a scanning rate of 100 mV s^{-1}.

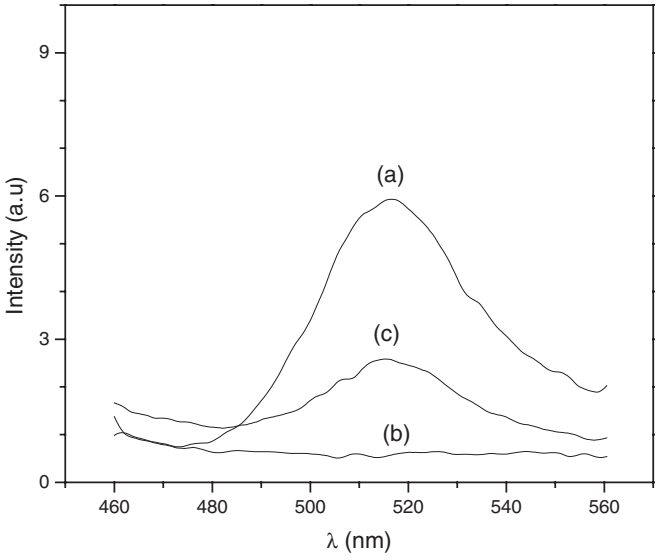

Figure 11. Fluorescence spectra of a) 4.0×10^{-9} M fluorescein cadaverin in water, b) the rinsing water from walls of the microcontainers sealed in the electrolyte solution containing fluorescein cadaverin, and c) an aqueous medium, in which the sealed and washed microcontainers were broken (excitation: 380 nm).

electrodeposited polypyrrole microcontainers on a stainless steel electrode in an aqueous solution of 0.5 M pyrrole and 0.4 M β-NSA in the presence of 1.0×10^{-6} M fluorescein cadaverin (as a fluorescence label) by cyclic voltammetric scanning from 0.5 to 1.2 V at a scanning rate of 20 mV s^{-1} for 5 cycles. After having sealed the microcontainers in situ in the polymerization solution, we then rinsed the electrode coated with the sealed polypyrrole microcontainers thoroughly with distilled water until there was no fluorescein cadaverin in the rinsing liquid, as detected using a fluorescence spectrometer. The closed microcontainers on the electrode were then squeezed in 2 mL distilled water by another hard surface (e.g., a pristine stainless steel plate) to break the microcontainers. As shown in Figure 11c, the fluorescence spectrum recorded from the water solution clearly shows fluorescence emission at 515 nm, characteristic of fluorescein cadaverin in water, indicating the encapsulation of fluorescein cadaverin within the sealed polypyrrole microcontainers.

3. Conclusion

We have demonstrated that conducting-polymer microcontainers can be prepared by electrochemical polymerization appropriate monomers using soap bubbles as a template. The process involves the generation of H_2 gas around the working electrode at a negative potential, followed by self-assembly of the soap bubbles on the working electrode and electrochemical polymerization of pyrrole along the wall of the soap bubbles under a positive potential. It was noticed that the density, shape, and wall thickness of polypyrrole microcontainers thus

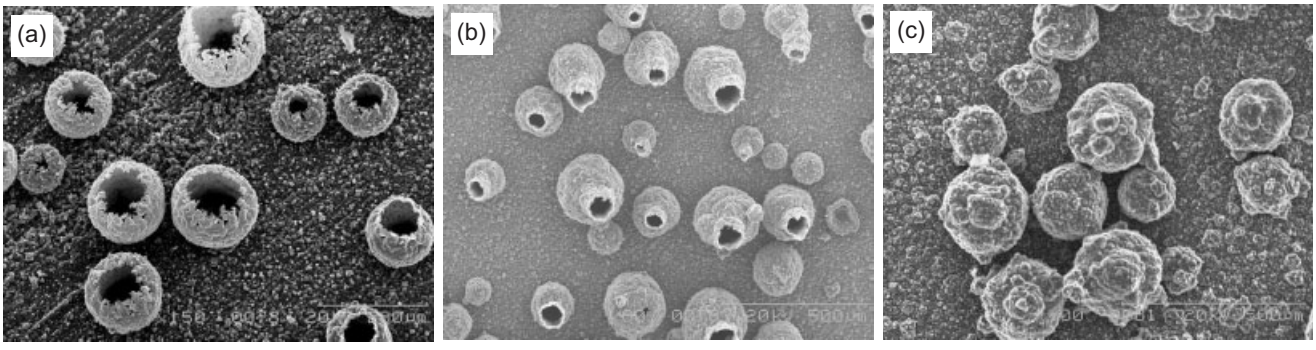

Figure 10. SEM images of a) semi-closed, b) partially, and c) fully sealed polypyrrole microcontainers. First, the template was formed by generating soap bubbles over a –1.0 to –1.65 V potential window, scanning rate 20 mV s^{-1}, 1 cycle. Then, polypyrrole was formed around the soap bubble template over a 0.5 to 1.1 V potential window for 3 cycles at a scanning rate 20 mV s^{-1} in an aqueous solution of 0.5 M pyrrole and 0.4 M β-NSA. Finally, the polypyrrole microcontainers thus prepared were closed in an aqueous solution of 0.5 M pyrrole and 0.4 M β-NSA by polymerizing pyrrole around the wall of the preformed microcontainers through cyclic voltammetric scanning over a 0.5 to 1.2 V potential window for b) 2 additional cycles and c) 5 additional cycles at a scanning rate 20 mV s^{-1} (scale bars: a) 200; b) 500; c) 500 μm). Note that the micrographs shown in (a–c) were not taken from the same spot due to technical difficulties.

ADVANCED FUNCTIONAL MATERIALS

prepared could be regulated by controlling the applied potentials both for the generation of H_2 gas and for the polymerization of pyrrole, concentration of electrolyte, cyclic voltammetric scan number, and scanning rate. By pre-patterning the working electrode surface with non-conducting polymers using μCP and plasma patterning, regio-specific electrochemical deposition of conducting-polymer microcontainers can be readily achieved. Furthermore, we have also demonstrated that the open mouth of the resulting conducting-polymer microcontainers can be sealed by sequential polymerization(s). Using a fluorescence-labeling method, we showed that these microcontainers could be used to encapsulate foreign objects. Therefore, the patterned and non-patterned conducting-polymer microcontainers with an open or closed mouth are very attractive for a wide range of potential applications, ranging from sensors to the controlled release of drugs.

4. Experimental

Chemicals and Characterization: Pyrrole (99 %) and 2-naphthalenesulfonic acid sodium salt (β-NSA, 99 %) were purchased from Acros. 5-(5-Aminopentyl thioureidyl) fluorescein dihydrobromide salt (fluorescein cadaverin, Fc) was purchased from Sigma. Scanning electron microscope images were taken using a Hitachi S-2150 SEM, and photoluminescence emissions were recorded using a LS 55 Luminescence Spectrometer (Perkin-Elmer, Inc.). Fourier-transform infrared, FTIR, measurements were performed on a Nexus 870 FT-IR Spectrometer (Thermo Spectra-Tech Inc.)

Preparation of Microcontainers: The electropolymerization of polypyrrole microcontainers was carried out on the CHI 604 electrochemical analyzer (HCH Instruments Inc.) in a 5 mL electrolyte cell at room temperature, using two stainless steel sheets (1 cm × 0.5 cm × 0.6 mm) as the working and counter electrodes and a Ag/AgCl electrode for reference. The working and counter electrodes were placed 0.5 cm apart in a 5 mL electrolyte cell containing an aqueous solution of pyrrole and β-NSA of predetermined concentrations; the latter was used both as the surfactant and electrolyte. Prior to the electropolymerization, the electrolyte solution was degassed with a pure nitrogen flow for 15 min and maintained at a slight overpressure throughout the electrochemical process. Cyclic voltammetric scan(s) were performed to generate H_2 bubbles on the working electrode surface by scanning the potential from –1.0 to –1.6 V for the first cycle, followed by changing the potential window to the range of 0.5 to 1.1 V for seven subsequent cycles for electrochemical polymerization of pyrrole around the "soap bubbles" on the working electrode. Electrodes with a pre-patterned non-conducting polymer layer were prepared using either μCP or plasma patterning. Electrochemical redox and fluorescence emission measurements were performed to demonstrate the potential uses of these conducting-polymer microcontainers for sensing and controlled-release applications. As reference, conventional polypyrrole films were electropolymerized in an aqueous solution of 0.1 M $NaClO_4$ and 0.25 M pyrrole on the steel electrode at a scan rate of 100 mV s^{-1} for 3 cycles over a potential range of 0.5 V to 1.1 V.

Received: July 26, 2003
Final version: October 10, 2003

[1] For recent reviews, see: a) S. N. Hanna, in *Handbook of Nanophase Materials* (Ed: A. N. Goldstein), Marcel Dekker, New York **1997**. b) F. Caruso, *Adv. Mater.* **2001**, *13*, 11. c) L. Dai, *Encyclopedia of Nanoscience and Nanotechnology* (Ed: H. S. Nalwa), American Scientific Publisher, CA, in press.
[2] A. V. Kabanov, V. P. Chekhonin, *Febs Lett.* **1989**, *258*, 343.
[3] L. Dai, D. H. Reneker, in *Nanowires* (Ed: Z. L. Wang), Kluwer Academic Pubulishers, Dordrecht, **2003**.
[4] A. A. Zakhidov, R. H. Baughman, Z. Iqbal, C. Cui, I. Khayrullin, S. O. Dantas, J. Marti, V. G. Ralchenko, *Science* **1998**, *282*, 897.
[5] C. R. Martin, *Acc. Chem. Res.* **1995**, *28*, 61.
[6] Z. Cai, C. R. Martin, *J. Am. Chem. Soc.* **1989**, *111*, 4138.
[7] L. Qu, G. Shi, F. Chen, J. Zhang, *Macromolecules* **2003**, *36*, 1063.
[8] L. Dai, *Radiat. Phys. Chem.* **2001**, *62*, 55.
[9] R. A. Jeong, G. J. Lee, H. S. Kim, K. Ahn, K. Lee, K. H. Kim, *Synth. Met.* **1998**, *98*, 9.
[10] *Tables of Spectral Data for Structure Determination of Organic Compounds*, 2nd ed., (Ed: W. Fresenius, J. F. K. Huber, E. Pungor, G. A. Rechnitz, W. Simon, T. S. West), Springer-Verlag, Berlin **1989**.
[11] R. J. Jackman, G. M. Whitesides, *CHEMTECH* **1999**, 18.
[12] L. Dai, H. J. Griesser, W. H. Mau, *J. Phys. Chem. B* **1997**, *101*, 9548.
[13] L. Dai, P. Soundarrajan, T. Kim, *Pure Appl. Chem.* **2002**, *74*, 1753.

